



Article

Doxorubicin-Conjugated PAMAM Dendrimers for pH-Responsive Drug Release and Folic Acid-Targeted Cancer Therapy

Mengen Zhang ¹, Jingyi Zhu ², Yun Zheng ¹, Rui Guo ¹ , Shige Wang ¹, Serge Mignani ³, Anne-Marie Caminade ⁴ , Jean-Pierre Majoral ⁴ and Xiangyang Shi ^{1,3,*}

¹ Key Laboratory of Science & Technology of Eco-Textile, Ministry of Education, College of Chemistry, Chemical Engineering and Biotechnology, Donghua University, Shanghai 201620, China; zhangmengen_163@163.com (M.Z.); zhengyun891869@163.com (Y.Z.); ruiguodhu.edu.cn (R.G.); sgwang@usst.edu.cn (S.W.)

² College of Materials Science and Engineering, Donghua University, Shanghai 201620, China; zhujy1210@163.com

³ Centro de Química da Madeira (CQM), Universidade da Madeira, Campus da Penteada, 9020-105 Funchal, Portugal; serge_mignani@orange.fr

⁴ Laboratoire de Chimie de Coordination du CNRS, 205 Route de Narbonne, BP 44099, 31077 Toulouse CEDEX 4, France; anne-marie.caminade@lcc-toulouse.fr (A.-M.C.); jean-pierre.majoral@lcc-toulouse.fr (J.-P.M.)

* Correspondence: xshi@dhu.edu.cn; Tel.: +86-216-779-2656

Received: 18 August 2018; Accepted: 17 September 2018; Published: 19 September 2018



Abstract: We present here the development of multifunctional doxorubicin (DOX)-conjugated poly(amidoamine) (PAMAM) dendrimers as a unique platform for pH-responsive drug release and targeted chemotherapy of cancer cells. In this work, we covalently conjugated DOX onto the periphery of partially acetylated and folic acid (FA)-modified generation 5 (G5) PAMAM dendrimers through a pH-sensitive *cis*-aconityl linkage to form the G5.NHAc-FA-DOX conjugates. The formed dendrimer conjugates were well characterized using different methods. We show that DOX release from the G5.NHAc-FA-DOX conjugates follows an acid-triggered manner with a higher release rate under an acidic pH condition (pH = 5 or 6, close to the acidic pH of tumor microenvironment) than under a physiological pH condition. Both *in vitro* cytotoxicity evaluation and cell morphological observation demonstrate that the therapeutic activity of dendrimer-DOX conjugates against cancer cells is absolutely related to the DOX drug released. More importantly, the FA conjugation onto the dendrimers allowed a specific targeting to cancer cells overexpressing FA receptors (FAR), and allowed targeted inhibition of cancer cells. The developed G5.NHAc-FA-DOX conjugates may be used as a promising nanodevice for targeted cancer chemotherapy.

Keywords: PAMAM dendrimer; doxorubicin; *cis*-aconityl linkage; pH-responsive release; targeted cancer therapy

1. Introduction

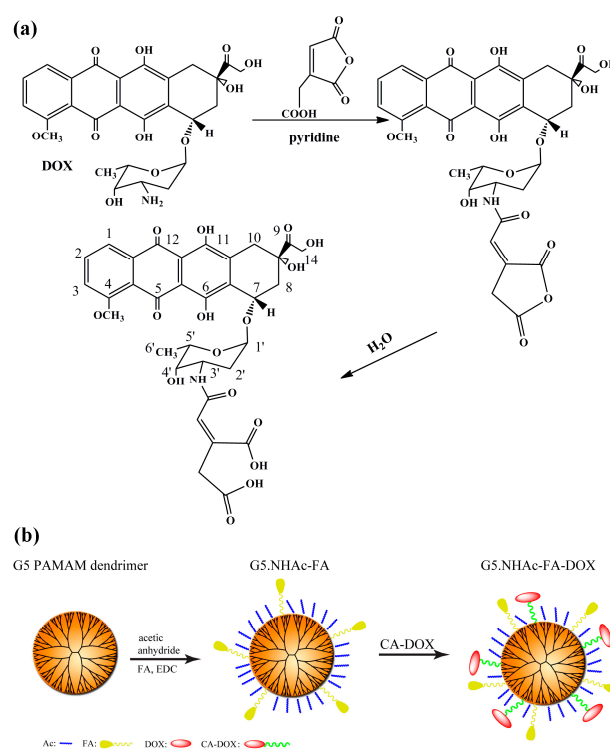
Anticancer therapy is usually associated with side-effects due to non-specific distribution of therapeutics in normal tissues. To achieve a better therapeutic efficacy, the use of a target-specific delivery, together with a stimuli-responsive nanocarrier system, offers an attractive strategy [1]. In addition to passive accumulation of drugs at tumor sites through enhanced permeability and retention (EPR) effect, an active targeting through the recognition between modified ligands on carriers and specific receptors on tumor tissues allows an enhanced drug accumulation at the site of

interest [2]. Moreover, a stimuli-responsive release to achieve a spatial, temporal, and dosage-controlled drug delivery exhibits unique advantages in current cancer therapy [3]. This is mainly because the drugs loaded within a carrier system is able to be released and localized within the tumor tissues upon the triggering by the tumor microenvironment such as low pH, hypoxia, or specific enzymatic conditions, etc.

Folic acid (FA)-linked therapeutic agents have been commonly used for selectively delivering drugs to cancer tissues expressing folate receptors (FAR) [4–6], which have been found to be overexpressed in many types of tumors [7,8], such as colon carcinoma, epidermoid carcinoma (KB), and ovarian carcinoma. Upon binding of FA ligands with FAR expressed onto the surface of cancer cells with a high affinity, the nanocarriers linked with FA can be subsequently internalized into cancer cells through the receptor-mediated endocytosis process and release the therapeutic agents to cancer cells in a specific manner [4,9–11]. Among the stimuli investigated for anticancer drug delivery, such as pH [12], temperature [13], and redox [14], pH has been usually investigated to trigger the drug release, since in solid tumors, the extracellular pH is more acidic (~6.5) than the physiological pH (~7.4) of normal tissue due to the irregular angiogenesis [15]. Regarding the applications of acid-triggered drug release, acid-sensitive linkage systems such as hydrazone bond [16,17] and *cis*-aconityl linkage [18,19] have been studied to design the stimuli-responsive drug delivery systems. For example, Chytil P. et al. [20] conjugated doxorubicin (DOX) to *N*-(2-hydroxypropyl) methacrylamide (HPMA) copolymers via a hydrazone bond, and demonstrated an enhanced anticancer activity of DOX in vitro and in vivo.

While liposomes [21], micelles [22], and polymer-based nanoparticles [23] have shown a significant improvement in tumor targeting therapy when incorporated with anticancer drugs, a drug carrier with collective merits of well-defined structure, uniform dispersity, water-solubility, and biocompatibility is extremely limited. Dendrimers, a class of branched, highly monodispersed, stepwise synthetic macromolecules with a well-defined composition and architecture, offer unique properties in applications of drug delivery [24–29]. The well-defined surface functional groups allow for conjugation with targeting ligands [30], therapeutic drugs [31], and imaging agents [32,33] for optimizing the drug delivery performance [34]. Moreover, dendrimers are considered as biocompatible and nonimmunogenic, and the size of dendrimers is small enough (e.g., G5 PAMAM dendrimers have a diameter of 5.4 nm) to allow them to be cleared from the blood through the kidney, solving the requirement of biodegradability [30,35]. PAMAM dendrimers, the most extensively studied dendrimers, have attracted great attention in a variety of biomedical applications including in vitro and in vivo drug delivery [36–38], gene delivery [39], and in vivo imaging [34,40] studies. In our previous work, we have demonstrated that targeting ligands such as FA or cyclic arginine-glycine-aspartic acid (RGD) peptide can be modified onto the surface of G5 PAMAM dendrimers for specific targeted delivery of physically encapsulated 2-methoxyestradiol [41], doxorubicin [42–44], or combretastatin A4 [45] to cancer cells expressing the corresponding receptors. In addition, FA and RGD-targeted dendrimer systems covalently linked with anticancer drug via a pH-sensitive linker have been designed for targeted drug delivery applications [46–48]. These prior studies highlight the importance of using dendrimers as a unique platform for targeted drug delivery applications, and also lead us to hypothesize that the FA-targeted stimuli-responsive delivery of anticancer drugs using a dendrimer-based system may be realized for cancer chemotherapy applications.

In this work, we synthesized partially acetylated G5 PAMAM dendrimers modified with a targeting agent FA and an imaging agent fluorescein isothiocyanate (FI) for the subsequent linking of DOX through a *cis*-aconityl linker for pH-responsive targeted drug delivery to cancer cells expressing FAR (Scheme 1). The synthesized multifunctional dendrimers were characterized and the pH-responsive drug release behavior was studied. The dendrimer-DOX conjugates were used for targeted delivery to cancer cells expressing FAR in vitro.



Scheme 1. Schematic illustration of the synthesis of (a) *Cis*-Aconityl-Doxorubicin (CA-DOX) and (b) G5.NHAc-FA-DOX conjugates. FA: folic acid; DOX: doxorubicin.

2. Materials and Methods

2.1. Synthesis of *Cis*-Aconityl-Doxorubicin (CA-DOX)

CA-DOX was synthesized according to the literature with some modifications [49,50]. As shown in Scheme 1, doxorubicin hydrochloride (DOX·HCl) (40 mg) was dissolved in 1 mL of pyridine, triethylamine (TEA) was then added to neutralize the hydrochloride of DOX·HCl. *Cis*-aconitic anhydride (40 mg) in dioxane (1 mL) was added slowly to the above DOX solution under magnetic stirring at 4 °C. After overnight reaction, the mixture was extracted by 5 mL of ethyl acetate and 5 mL of 5% aqueous sodium bicarbonate solution (2–3 times). The aqueous phase was collected and cooled to 4 °C. The pH of the aqueous solution was carefully adjusted with 1.0 M HCl under vigorous stirring until the formation of a precipitate, and the pH of the acidified solution was 2.5–3.0. Through centrifugation of the precipitate at 4 °C (7000 rpm, 10 min), washing, and lyophilization, CA-DOX was obtained.

2.2. Synthesis of Functional G5 Dendrimers and Conjugates

According to the protocols reported in the literature [41,45], the surface amines of the G5.NH₂ dendrimers were partially converted to acetamide groups by reacting with acetic anhydride to form G5.NHAc, then the products were further conjugated with FA, FI, or FA and FI to form G5.NHAc-FA, G5.NHAc-FI, or G5.NHAc-FA-FI dendrimers. These synthesized products were characterized by ¹H NMR and UV-vis spectroscopy using our previously reported procedures [41].

To synthesize the G5.NHAc-FA-DOX conjugates, the aqueous sodium bicarbonate solution of CA-DOX was not acidified to pH 2.5–3.0 but to pH 6.0 with no precipitation, then 1-ethyl-3-[3-dimethylaminopropyl] carbodiimide hydrochloride (EDC) and N-hydroxysuccinimide (NHS) were added to the solution to activate the CA-DOX for 30 min. After that, G5.NHAc-FA dendrimers (30 molar equiv.) in 2 mL of water was added to the solution of activated CA-DOX under stirring overnight in the dark at room temperature with an immediate

adjustment of pH to 8.0. The synthesized product was purified by gel ultrafiltration via a Sephadex G-25 gel column (GE Healthcare Life Sciences, Pittsburgh, PA, USA). The product was collected, ultrafiltered, and lyophilized to obtain the final G5.NHAc-FA-DOX conjugates. See more experimental details in Supplementary Materials.

3. Results and Discussion

3.1. Synthesis and Characterization of Dendrimer-DOX Conjugates

To prepare the dendrimer-based drug delivery platform, we first partially acetylated the G5 PAMAM dendrimer peripheral amine groups, and then sequentially conjugated FA and FI as the specific targeting and imaging agents, respectively. Both ^1H NMR (Figure S1, Supplementary Materials) and UV-vis spectroscopy (Figure 1) demonstrates the success of the conjugation of FI and FA moieties with the terminal dendrimer amine groups, in accordance with our previous study [41]. Through the integration of the related ^1H NMR peaks, the average numbers of acetyl groups, FA and FI attached to each dendrimer were calculated to be 70, 4.5, and 5.0, respectively. In the UV-vis spectrum, the pristine G5.NH₂ dendrimers just display aliphatic absorption feature, and after FA conjugation, the typical absorption peak of FA at 280 nm can be clearly seen, further demonstrating the success of FA conjugation. Based on previous studies, five of FA or FI moieties attached onto the surface of each dendrimer are adequate for cancer cell targeting through receptor-mediated manner and for detecting cancer cell via the fluorescence-based analytical techniques [51].

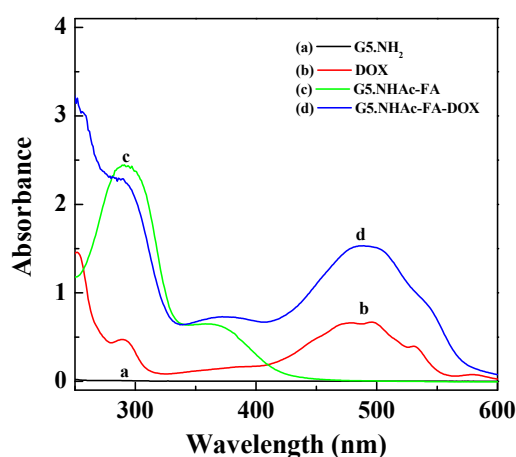


Figure 1. UV-vis spectra of G5.NH₂ dendrimers, DOX·HCl, G5.NHAc-FA dendrimers, and G5.NHAc-FA-DOX conjugates in aqueous solution.

To link DOX to the surface of G5 PAMAM dendrimers via a pH-responsive linker, we first prepared CA-DOX by reacting the amine group of DOX with *cis*-aconitic anhydride (Scheme 1a). The structure of CA-DOX was identified by ^1H NMR (Figure 2). ^1H NMR spectrum shows that the emergence of two peaks at 6.47 ppm and 14 ppm is related to the protons of =CH-CO- and carboxyl groups of the *cis*-aconitic anhydride linkage, respectively. The aromatic proton peaks can be attributed to the characteristic DOX proton peaks (peaks 1–3), which is in a good agreement with the literature [49]. The successful synthesis of CA-DOX was further characterized by FTIR spectroscopy (Figure S2, Supplementary Materials). In comparison with the FTIR spectrum of DOX, CA-DOX shows a broad band stretching across 3000 cm⁻¹, which is assigned to the formation of the -COOH group for the *cis*-aconitic anhydride linkage. CA-DOX was also characterized by HPLC (Figure S3, Supplementary Materials). The retention time of DOX is 11 min, while the retention time of CA-DOX is 4.6 min, and still a small portion of unreacted DOX was observed after purification.

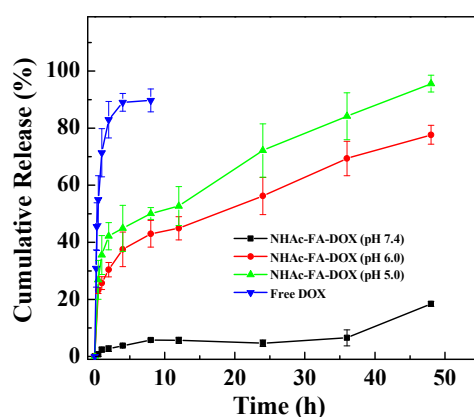


Figure 3. In vitro release profiles of DOX from G5.NHAc-FA-DOX conjugates in citrate buffer solutions (pH 7.4, pH 6.0, and pH 5.0) and the release of free DOX·HCl in citrate buffer solution (pH 7.4) at 37 °C.

3.3. In Vitro Cytotoxicity Assay

To evaluate the pharmacological activity of dendrimer-DOX conjugates, in vitro MTT cytotoxicity tests against KB cells were performed. The cytotoxicity of G5 PAMAM dendrimers and modified dendrimers (G5.NH₂, G5.NHAc, and G5.NHAc-FA) were determined prior to the cytotoxicity tests of dendrimer-DOX conjugates. Figure 4 shows the viability of KB cells treated with G5.NH₂, G5.NHAc and G5.NHAc-FA dendrimers at different concentrations. When the concentration of G5.NH₂ was increased to 1 μM, the viability of KB cells was as low as 55%, and the cells reached a viability of approximately 10% at a dendrimer concentration of 5 μM, indicating the cytotoxicity of G5.NH₂ dendrimers, similar to our previous work [52]. In contrast, the cell viability remains more than 80% after the cells were treated by both modified dendrimers (G5.NHAc and G5.NHAc-FA) at a concentration of 1 μM. No significant cytotoxicity was observed when the concentration of modified dendrimers reached up to 20 μM, indicating that the dendrimer toxicity can be significantly alleviated after surface acetylation modification.

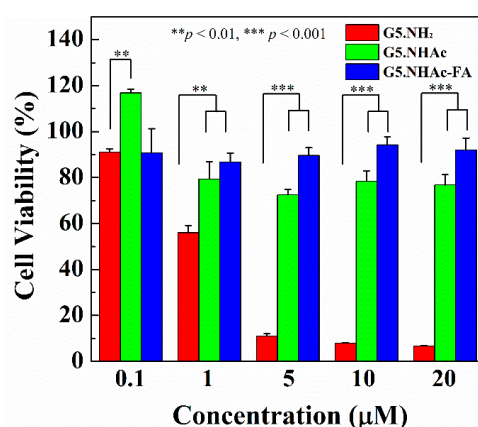


Figure 4. The viability of KB cells treated with G5.NH₂, G5.NHAc, and G5.NHAc-FA dendrimers at different concentrations.

Figure 5 shows the variation of cell viability after 48 h of treatment by free DOX, G5.NHAc-DOX and G5.NHAc-FA-DOX. The IC₅₀ value of free DOX was determined to be 0.3 μM, whereas the IC₅₀ values of G5.NHAc-DOX and G5.NHAc-FA-DOX were measured to be 19 μM and 4 μM, respectively. These results indicate that dendrimer-DOX conjugates exhibit a lower cytotoxicity against KB cells than free DOX. This may be because the release of DOX from dendrimer-DOX conjugates was not completed after endocytosis, and only a portion of DOX exerted the therapeutic function. It should

be also noticed that conjugation of FA moieties onto the dendrimers affords a decreased IC_{50} value of dendrimer-DOX conjugates from 19 μM to 4 μM , indicating an improvement of the antitumor efficiency after FA modification. This could be due to the FA-rendered targeting specificity to cancer cells expressing FAR (see below). The cytotoxicity of the G5.NHAc-DOX conjugates was further verified by visual observation of the morphology change of KB cells after 48 h of incubation (Figure S4, Supplementary Materials).

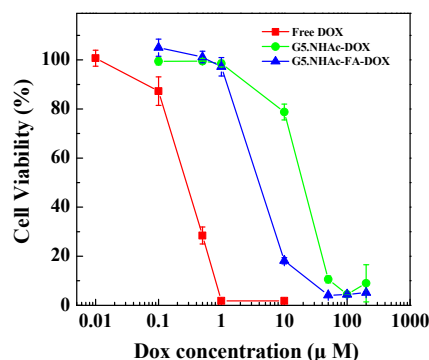


Figure 5. In vitro cytotoxicity of free DOX, G5.NHAc-DOX conjugates, and G5.NHAc-FA-DOX conjugates against KB cells.

3.4. Cellular Uptake of Dendrimer-DOX Conjugates

Flow cytometry assay was carried out to analyze the cellular uptake of dendrimer-DOX conjugates by KB cells by detecting the fluorescence intensity of cells after incubation with G5.NHAc-DOX and G5.NHAc-FA-DOX with a DOX concentration of 40 μM for 2.5 h at 37 °C. Free DOX at a concentration of 10 μM was also tested for comparison. As shown in Figure 6a, a significant increase in cell fluorescence was observed after KB cells were treated with free DOX and dendrimer-DOX conjugates. In general, the fluorescent intensity of free DOX is higher than that of the dendrimer-DOX conjugates even though the tested concentration of free DOX is lower than that of DOX in dendrimer-DOX conjugates. This suggests that the uptake of free DOX is faster than that of dendrimer-DOX conjugates by KB cells. It should also be noted that the cellular uptake of G5.NHAc-FA-DOX conjugate was remarkably higher than that of G5.NHAc-DOX conjugates ($p < 0.01$, Figure 6b), which means that FA-mediated binding process was involved in the cellular uptake of G5.NHAc-FA-DOX. The higher cellular uptake of G5.NHAc-FA-DOX could also explain the higher cytotoxicity of G5.NHAc-FA-DOX vs. G5.NHAc-DOX (Figure 5). Taken together, the flow cytometry study strongly reveals that the introduction of FA moiety to the surface of dendrimers allows for specific targeting of KB cells overexpressing FAR.

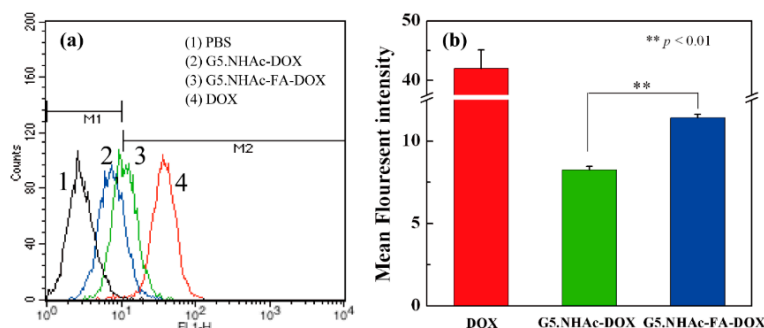


Figure 6. Flow cytometry analysis of (a) the in vitro cellular uptake of free DOX (10 μM), G5.NHAc-DOX and G5.NHAc-FA-DOX with a DOX concentration of 40 μM in KB cells after 2.5 h incubation and (b) the mean fluorescence intensity of KB cells after 2.5 h treatment. KB cells treated with PBS were set as control.

The FA-mediated targeting specificity for dendrimer-DOX conjugates to FAR-expressing cancer cells was further confirmed by confocal microscopic analysis (Figure 7). FI was labeled to the G5.NHAc-FA-DOX conjugates to detect the cellular uptake and internalization of the dendrimer-DOX conjugates. As displayed in Figure 7, free DOX was localized in the cell nuclei with a red fluorescence signal (Figure 7b), which were also counterstained with Hoechst 33342 in a blue fluorescence, hence showing a pink fluorescence signal in the merged image. When KB-HFAR cells were treated with FI-labeled dendrimer-DOX conjugates, the G5.NHAc-FA-FI-DOX group displayed a stronger fluorescence signal (Figure 7d) than the G5.NHAc-FI-DOX group (Figure 7c), which was associated with an increased cellular uptake of the G5.NHAc-FA-FI-DOX conjugates. Under the same imaging conditions, KB cells having low-level of FAR expression (KB-LFAR) cells displayed a weaker fluorescence signal (Figure 7e) than KB cells having high-level of FAR expression (KB-HFAR) cells (Figure 7d) when treated with G5.NHAc-FA-FI-DOX conjugate. Additionally, the fluorescence of dendrimer-DOX conjugates distributed within the entire cell, which is likely due to the readily release of DOX in acidic lysosomes and a following entrance into cell nuclei, in agreement with previous reports [8,37]. The confocal microscopic analysis suggests that the cellular uptake of FA-modified dendrimer-DOX conjugates is largely related to FAR-mediated endocytosis process, and FA-modified dendrimer-DOX conjugates are capable of specifically targeting KB-HFAR cells.

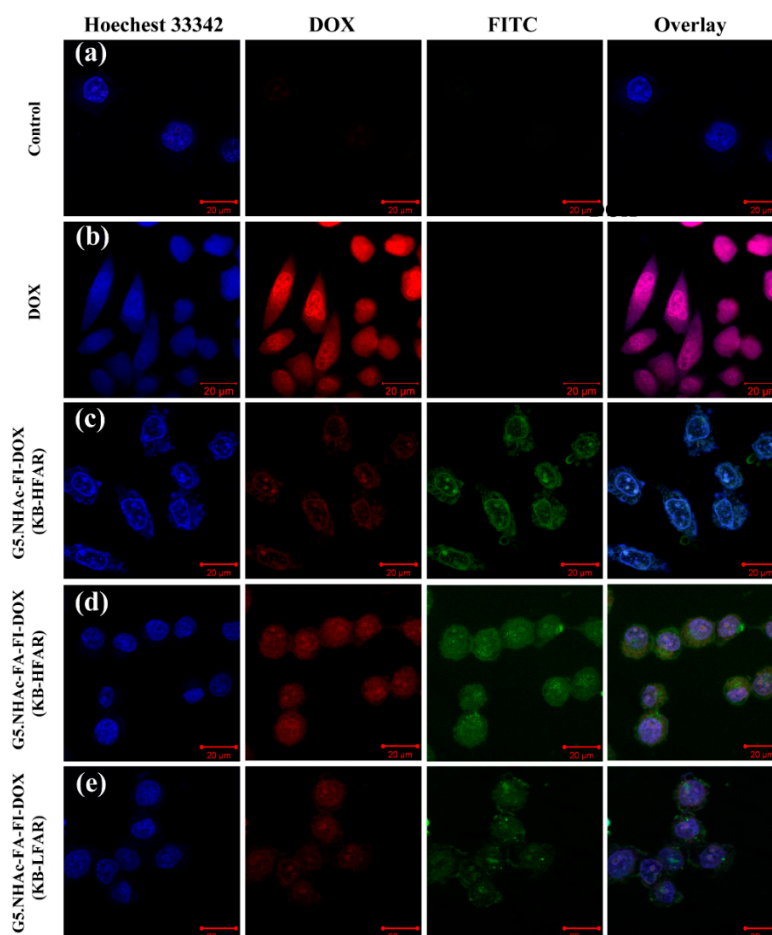


Figure 7. Confocal laser scanning microscopic images of KB cells having high-level of FAR expression (KB-HFAR) cells treated with (a) PBS, (b) free DOX (10 μ M), (c) G5.NHAc-FI-DOX (40 μ M DOX-equiv.), (d) G5.NHAc-FA-FI-DOX (40 μ M DOX-equiv.), and (e) KB cells having low-level of FAR expression (KB-LFAR) cells treated with G5.NHAc-FA-FI-DOX (40 μ M DOX-equiv.).

3.5. Targeted Antitumor Efficacy of G5.NHAc-FA-DOX Conjugates

The targeted inhibition effect of FA-modified dendrimer-DOX conjugates on FAR-overexpressing KB cells was verified by the MTT assay. Figure 8 shows the viability of KB-HFAR and KB-LFAR cells treated with dendrimer-DOX conjugates. The incubation of KB-HFAR cells with the G5.NHAc-FA-DOX conjugates caused a significant loss (87.6%) of cell viability ($p < 0.01$ vs. control). In contrast, KB-LFAR cells displayed a viability of 76.1% after the same treatment with the G5.NHAc-FA-DOX conjugate. It should also be noted that KB-HFAR cells only lost 25.4% of viability after the treatment with G5.NHAc-DOX conjugates. Taken together, the results fully imply that the G5.NHAc-FA-DOX conjugates enable a specific targeted inhibition of cancer cells via FAR-mediated endocytosis.

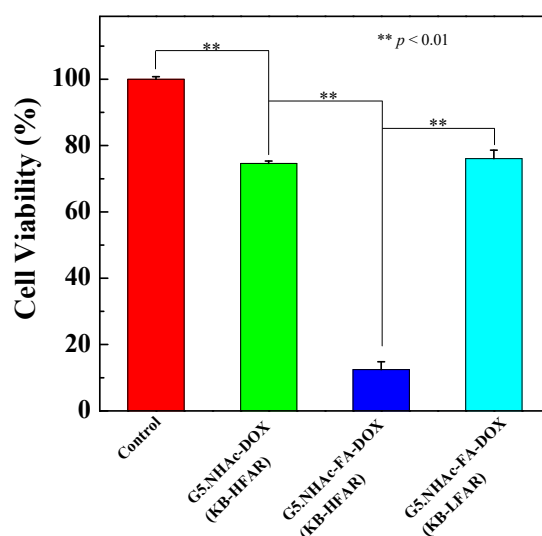


Figure 8. MTT assay of the viability of KB-HFAR cells treated with G5.NHAc-FA-DOX conjugates or G5.NHAc-DOX conjugates and KB-LFAR cells treated with G5.NHAc-FA-DOX with a DOX concentration of 50 μ M at 37 °C for 2 h.

The use of pH-triggered release of drug together with the active targeting of FA ligand in the G5.NHAc-FA-DOX holds several advantages over other schemes. First, to compare with the physical encapsulation of DOX [43], DOX conjugated onto dendrimers via acid-sensitive linkage can be released in a more controlled manner. Rare DOX was released at pH 7.4, which minimize the release of drug during blood circulation. Second, the IC_{50} value of DOX in G5.NHAc-FA-DOX against KB cells was approximately 4 μ M, which is much lower than that in other DOX-dendrimer conjugate (12.95 μ M) against murine B16 melanoma cells [18].

4. Conclusions

In summary, a multifunctional G5 PAMAM dendrimer-based drug delivery system was prepared by linking FA-modified and partially acetylated G5 dendrimers with DOX through a *cis*-aconityl linkage for targeted drug delivery to FAR-expressing cancer cells. The introduced *cis*-aconityl linkage rendered the dendrimer-DOX conjugates with a pH-responsive release of DOX with a high DOX release rate at an acidic pH condition. The designed G5.NHAc-FA-DOX conjugates are capable of specifically targeting cancer cells via FAR-mediated endocytosis, and exhibiting a significantly enhanced therapeutic efficacy. With a unique capacity to covalently conjugate cancer drugs and to endow drugs with a controlled release and specific targeting properties, we anticipate that this multifunctional dendrimer-based drug delivery system may be used for targeted chemotherapy of cancer.

Supplementary Materials: The following are available online at <http://www.mdpi.com/1999-4923/10/3/162/s1>, Figure S1: ¹H NMR spectrum of G5.NHAc-FA dendrimers, Figure S2: FTIR spectra of DOX and CA-DOX, Figure S3: HPLC chromatograms of (a) DOX·HCl and (b) CA-DOX, Figure S4: Phase contrast microscopic images of KB cells treated with (a) 10 μL PBS, (b) G5.NHAc-DOX conjugates in 10 μL PBS (50 μM DOX-equiv), (c) G5.NHAc-FA-DOX conjugates in 10 μL PBS buffer (50 μM DOX-equiv), (d) free DOX in 10 μL PBS (1 μM), and (e) G5.NHAc-FA dendrimers in 10 μL PBS, respectively.

Author Contributions: Conceptualization, R.G. and X.S.; Methodology, X.S. and M.Z.; Validation, M.Z., J.Z., Y.Z., and S.W.; Formal Analysis, M.Z.; Data Curation, M.Z.; Writing-Original Draft Preparation, M.Z.; Writing-Review & Editing, S.M., A.-M.C., J.-P.M., and X. S.; Supervision, X.S.; Funding Acquisition, X.S.

Funding: This research is financially supported by the National Natural Science Foundation of China (81761148028, 21773026 and 21875031), the Science and Technology Commission of Shanghai Municipality (15520711400 and 17540712000), the Fundamental Research Funds for the Central Universities, and the Sino-French Caiyuanpei Programme. X. Shi and S. Mignani also thank the support of Fundação para a Ciência e a Tecnologia (FCT) with Portuguese Government funds through the CQM Strategic Project PEst-OE/QUI/UI0674/2013 and the Madeira 14–20 Program, project PROEQUIPRAM—Reforço do Investimento em Equipamentos e Infraestruturas Científicas na RAM (M1420-01-0145-FEDER-000008). ARDITI—Agência Regional para o Desenvolvimento da Investigação Tecnologia e Inovação is also acknowledged through the project M1420-01-0145-FEDER-000005—CQM+ (Madeira 14–20 Program).

Conflicts of Interest: The authors declare no conflict of interest.

References

1. Torchilin, V.P. Targeted pharmaceutical nanocarriers for cancer therapy and imaging. *AAPS J.* **2007**, *9*, E128–E147. [[CrossRef](#)] [[PubMed](#)]
2. Byrne, J.; Betancourt, T.; Brannon-Peppas, L. Active targeting schemes for nanoparticle systems in cancer therapeutics. *Adv. Drug Deliv. Rev.* **2008**, *60*, 1615–1626. [[CrossRef](#)] [[PubMed](#)]
3. Mura, S.; Nicolas, J.; Couvreur, P. Stimuli-responsive nanocarriers for drug delivery. *Nat. Mater.* **2013**, *12*, 991–1003. [[CrossRef](#)] [[PubMed](#)]
4. Low, P.S.; Henne, W.A.; Doorneweerd, D.D. Discovery and development of folic-acid-based receptor targeting for imaging and therapy of cancer and inflammatory diseases. *Acc. Chem. Res.* **2007**, *41*, 120–129. [[CrossRef](#)] [[PubMed](#)]
5. Majoros, I.J.; Myc, A.; Thomas, T.; Mehta, C.B.; Baker, J.R., Jr. Pamam dendrimer-based multifunctional conjugate for cancer therapy: Synthesis, characterization, and functionality. *Biomacromolecules* **2006**, *7*, 572–579. [[CrossRef](#)] [[PubMed](#)]
6. Gabizon, A.; Shmeeda, H.; Horowitz, A.T.; Zalipsky, S. Tumor cell targeting of liposome-entrapped drugs with phospholipid-anchored folic acid-peg conjugates. *Adv. Drug Deliv. Rev.* **2004**, *56*, 1177–1192. [[CrossRef](#)] [[PubMed](#)]
7. Weitman, S.D.; Weinberg, A.G.; Coney, L.R.; Zurawski, V.R.; Jennings, D.S.; Kamen, B.A. Cellular localization of the folate receptor: Potential role in drug toxicity and folate homeostasis. *Cancer Res.* **1992**, *52*, 6708–6711. [[PubMed](#)]
8. Goren, D.; Horowitz, A.T.; Tzemach, D.; Tarshish, M.; Zalipsky, S.; Gabizon, A. Nuclear delivery of doxorubicin via folate-targeted liposomes with bypass of multidrug-resistance efflux pump. *Clin. Cancer Res.* **2000**, *6*, 1949–1957. [[PubMed](#)]
9. Zhou, B.; Xiong, Z.; Wang, P.; Peng, C.; Shen, M.; Mignani, S.; Majoral, J.-P.; Shi, X. Targeted tumor dual mode CT/MR imaging using multifunctional polyethylenimine-entrapped gold nanoparticles loaded with gadolinium. *Drug Deliv.* **2018**, *25*, 178–186. [[CrossRef](#)] [[PubMed](#)]
10. Zhou, B.; Zhao, L.; Shen, M.; Zhao, J.; Shi, X. A multifunctional polyethylenimine-based nanoplatform for targeted anticancer drug delivery to tumors in vivo. *J. Mater. Chem. B* **2017**, *5*, 1542–1550. [[CrossRef](#)]
11. Zhu, J.; Zheng, L.; Wen, S.; Tang, Y.; Shen, M.; Zhang, G.; Shi, X. Targeted cancer theranostics using alpha-tocopheryl succinate-conjugated multifunctional dendrimer-entrapped gold nanoparticles. *Biomaterials* **2014**, *35*, 7635–7646. [[CrossRef](#)] [[PubMed](#)]
12. Gillies, E.R.; Jonsson, T.B.; Fréchet, J.M. Stimuli-responsive supramolecular assemblies of linear-dendritic copolymers. *J. Am. Chem. Soc.* **2004**, *126*, 11936–11943. [[CrossRef](#)] [[PubMed](#)]
13. Türk, M.; Dinçer, S.; Yuluğ, I.G.; Pişkin, E. In vitro transfection of hela cells with temperature sensitive polycationic copolymers. *J. Control. Release* **2004**, *96*, 325–340. [[CrossRef](#)] [[PubMed](#)]

14. Trachootham, D.; Alexandre, J.; Huang, P. Targeting cancer cells by ros-mediated mechanisms: A radical therapeutic approach? *Nat. Rev. Drug Discov.* **2009**, *8*, 579–591. [[CrossRef](#)] [[PubMed](#)]
15. Vaupel, P.; Kallinowski, F.; Okunieff, P. Blood flow, oxygen and nutrient supply, and metabolic microenvironment of human tumors: A review. *Cancer Res.* **1989**, *49*, 6449–6465. [[PubMed](#)]
16. Prabakaran, M.; Grailer, J.J.; Pilla, S.; Steeber, D.A.; Gong, S. Amphiphilic multi-arm-block copolymer conjugated with doxorubicin via ph-sensitive hydrazone bond for tumor-targeted drug delivery. *Biomaterials* **2009**, *30*, 5757–5766. [[CrossRef](#)] [[PubMed](#)]
17. Yuan, H.; Luo, K.; Lai, Y.; Pu, Y.; He, B.; Wang, G.; Wu, Y.; Gu, Z. A novel poly (L-glutamic acid) dendrimer based drug delivery system with both ph-sensitive and targeting functions. *Mol. Pharm.* **2010**, *7*, 953–962. [[CrossRef](#)] [[PubMed](#)]
18. Zhu, S.; Hong, M.; Tang, G.; Qian, L.; Lin, J.; Jiang, Y.; Pei, Y. Partly pegylated polyamidoamine dendrimer for tumor-selective targeting of doxorubicin: The effects of pegylation degree and drug conjugation style. *Biomaterials* **2010**, *31*, 1360–1371. [[CrossRef](#)] [[PubMed](#)]
19. Srinophakun, T.; Boonmee, J. Preliminary study of conformation and drug release mechanism of doxorubicin-conjugated glycol chitosan, via *cis*-aconityl linkage, by molecular modeling. *Int. J. Mol. Sci.* **2011**, *12*, 1672–1683. [[CrossRef](#)] [[PubMed](#)]
20. Chytil, P.; Etrych, T.; Kříž, J.; Šubr, V.; Ulbrich, K. *N*-(2-hydroxypropyl) methacrylamide-based polymer conjugates with ph-controlled activation of doxorubicin for cell-specific or passive tumour targeting. Synthesis by raft polymerisation and physicochemical characterisation. *Eur. J. Pharm. Sci.* **2010**, *41*, 473–482. [[CrossRef](#)] [[PubMed](#)]
21. Andresen, T.L.; Jensen, S.S.; Jørgensen, K. Advanced strategies in liposomal cancer therapy: Problems and prospects of active and tumor specific drug release. *Prog. Lipid Res.* **2005**, *44*, 68–97. [[CrossRef](#)] [[PubMed](#)]
22. Yang, X.; Grailer, J.J.; Pilla, S.; Steeber, D.A.; Gong, S. Tumor-targeting, ph-responsive, and stable unimolecular micelles as drug nanocarriers for targeted cancer therapy. *Bioconjugate Chem.* **2010**, *21*, 496–504. [[CrossRef](#)] [[PubMed](#)]
23. Brannon-Peppas, L.; Blanchette, J.O. Nanoparticle and targeted systems for cancer therapy. *Adv. Drug Deliv. Rev.* **2012**, *64*, 206–212. [[CrossRef](#)]
24. Tomalia, D.A.; Naylor, A.M.; Goddard, W.A. Starburst dendrimers: Molecular-level control of size, shape, surface chemistry, topology, and flexibility from atoms to macroscopic matter. *Angew. Chem.-Int. Edit.* **1990**, *29*, 138–175. [[CrossRef](#)]
25. Mignani, S.; Rodrigues, J.; Tomas, H.; Zabolcka, M.; Shi, X.; Caminade, A.-M.; Majoral, J.-P. Dendrimers in combination with natural products and analogues as anti-cancer agents. *Chem. Soc. Rev.* **2018**, *47*, 514–532. [[CrossRef](#)] [[PubMed](#)]
26. Fan, Y.; Sun, W.; Shi, X. Design and biomedical applications of poly(amidoamine)-dendrimer-based hybrid nanoarchitectures. *Small Methods* **2017**, *1*, 1700224. [[CrossRef](#)]
27. Kim, Y.; Park, E.; Na, D. Recent progress in dendrimer-based nanomedicine development. *Arch. Pharm. Res.* **2018**, *41*, 571–582. [[CrossRef](#)] [[PubMed](#)]
28. Lu, J.; Li, N.; Gao, Y.; Li, N.; Guo, Y.; Liu, H.; Chen, X.; Zhu, C.; Dong, Z.; Yamamoto, A. The effect of absorption-enhancement and the mechanism of the pamam dendrimer on poorly absorbable drugs. *Molecules* **2018**, *23*, 2001. [[CrossRef](#)] [[PubMed](#)]
29. Spyropoulos-Antonakakis, N.; Sarantopoulou, E.; Trohopoulos, P.N.; Stefi, A.L.; Kollia, Z.; Gavriil, V.E.; Bourkoula, A.; Petrou, P.S.; Kakabakos, S.; Semashko, V.V.; et al. Selective aggregation of pamam dendrimer nanocarriers and PAMAM/ZNPC nanodrugs on human atheromatous carotid tissues: A photodynamic therapy for atherosclerosis. *Nanoscale Res. Lett.* **2015**, *10*, 210. [[CrossRef](#)] [[PubMed](#)]
30. Shukla, R.; Thomas, T.P.; Peters, J.; Kotlyar, A.; Myc, A.; Baker, J.R., Jr. Tumor angiogenic vasculature targeting with pamam dendrimer-rgd conjugates. *Chem. Commun.* **2005**, *0*, 5739–5741. [[CrossRef](#)] [[PubMed](#)]
31. Gurdag, S.; Khandare, J.; Stapels, S.; Matherly, L.H.; Kannan, R.M. Activity of dendrimer-methotrexate conjugates on methotrexate-sensitive and-resistant cell lines. *Bioconjugate Chem.* **2006**, *17*, 275–283. [[CrossRef](#)] [[PubMed](#)]
32. Choi, Y.; Thomas, T.; Kotlyar, A.; Islam, M.T.; Baker, J.R., Jr. Synthesis and functional evaluation of DNA-assembled polyamidoamine dendrimer clusters for cancer cell-specific targeting. *Chem. Biol.* **2005**, *12*, 35–43. [[CrossRef](#)] [[PubMed](#)]

33. Hong, S.; Bielinska, A.U.; Mecke, A.; Keszler, B.; Beals, J.L.; Shi, X.; Balogh, L.; Orr, B.G.; Baker Jr, J.R.; Banaszak Holl, M.M. Interaction of poly (amidoamine) dendrimers with supported lipid bilayers and cells: Hole formation and the relation to transport. *Bioconjugate Chem.* **2004**, *15*, 774–782. [[CrossRef](#)] [[PubMed](#)]
34. Qiao, Z.; Shi, X. Dendrimer-based molecular imaging contrast agents. *Prog. Polym. Sci.* **2015**, *44*, 1–27. [[CrossRef](#)]
35. Peer, D.; Karp, J.M.; Hong, S.; Farokhzad, O.C.; Margalit, R.; Langer, R. Nanocarriers as an emerging platform for cancer therapy. *Nat. Nanotech.* **2007**, *2*, 751–760. [[CrossRef](#)] [[PubMed](#)]
36. Kurtoglu, Y.E.; Navath, R.S.; Wang, B.; Kannan, S.; Romero, R.; Kannan, R.M. Poly (amidoamine) dendrimer–drug conjugates with disulfide linkages for intracellular drug delivery. *Biomaterials* **2009**, *30*, 2112–2121. [[CrossRef](#)] [[PubMed](#)]
37. Lai, P.; Lou, P.; Peng, C.; Pai, C.; Yen, W.; Huang, M.; Young, T.; Shieh, M. Doxorubicin delivery by polyamidoamine dendrimer conjugation and photochemical internalization for cancer therapy. *J. Control. Release* **2007**, *122*, 39–46. [[CrossRef](#)] [[PubMed](#)]
38. He, H.; Li, Y.; Jia, X.; Du, J.; Ying, X.; Lu, W.; Lou, J.; Wei, Y. Pegylated poly (amidoamine) dendrimer-based dual-targeting carrier for treating brain tumors. *Biomaterials* **2011**, *32*, 478–487. [[CrossRef](#)] [[PubMed](#)]
39. Kong, L.; Alves, C.S.; Hou, W.; Qiu, J.; Moehwald, H.; Tomas, H.; Shi, X. Rgd peptide-modified dendrimer-entrapped gold nanoparticles enable highly efficient and specific gene delivery to stem cells. *ACS Appl. Mater. Interfaces* **2015**, *7*, 4833–4843. [[CrossRef](#)] [[PubMed](#)]
40. Peng, C.; Zheng, L.; Chen, Q.; Shen, M.; Guo, R.; Wang, H.; Cao, X.; Zhang, G.; Shi, X. Pegylated dendrimer-entrapped gold nanoparticles for in vivo blood pool and tumor imaging by computed tomography. *Biomaterials* **2012**, *33*, 1107–1119. [[CrossRef](#)] [[PubMed](#)]
41. Wang, Y.; Guo, R.; Cao, X.; Shen, M.; Shi, X. Encapsulation of 2-methoxyestradiol within multifunctional poly(amidoamine) dendrimers for targeted cancer therapy. *Biomaterials* **2011**, *32*, 3322–3329. [[CrossRef](#)] [[PubMed](#)]
42. He, X.; Alves, C.S.; Oliveira, N.; Rodrigues, J.; Zhu, J.; Bányai, I.; Tomás, H.; Shi, X. Rgd peptide-modified multifunctional dendrimer platform for drug encapsulation and targeted inhibition of cancer cells. *Colloids Surf. B Biointerfaces* **2015**, *125*, 82–89. [[CrossRef](#)] [[PubMed](#)]
43. Wang, Y.; Cao, X.; Guo, R.; Shen, M.; Zhang, M.; Zhu, M.; Shi, X. Targeted delivery of doxorubicin into cancer cells using a folic acid–dendrimer conjugate. *Polym. Chem.* **2011**, *2*, 1754–1760. [[CrossRef](#)]
44. Zhang, M.; Shi, X. Folic acid-modified dendrimer–dox conjugates for targeting cancer chemotherapy. *J. Control. Release* **2013**, *1*, e55–e56. [[CrossRef](#)]
45. Zhang, M.; Guo, R.; Wang, Y.; Cao, X.; Shen, M.; Shi, X. Multifunctional dendrimer/combretastatin a4 inclusion complexes enable in vitro targeted cancer therapy. *Int. J. Nanomed.* **2011**, *6*, 2337–2349.
46. Zhang, L.; Zhu, S.; Qian, L.; Pei, Y.; Qiu, Y.; Jiang, Y. Rgd-modified PEG–PAMAM–DOX conjugates: In vitro and in vivo studies for glioma. *Eur. J. Pharm. Biopharm.* **2011**, *79*, 232–240. [[CrossRef](#)] [[PubMed](#)]
47. Zhu, S.; Qian, L.; Hong, M.; Zhang, L.; Pei, Y.; Jiang, Y. Rgd-modified PEG–PAMAM–DOX conjugate: In vitro and in vivo targeting to both tumor neovascular endothelial cells and tumor cells. *Adv. Mater.* **2011**, *23*, H84–H89. [[CrossRef](#)] [[PubMed](#)]
48. Hu, Q.; Ji, P.; Huang, F.; Zhu, Y.; Cheng, L.; Cheng, L.; Chen, D. Synthesis and characterization of fa modified pH-sensitive PAMAM doxorubicin conjugates. *J. China Pharm.* **2013**, *24*, 2350–2352.
49. Hu, F.; Liu, L.; Du, Y.; Yuan, H. Synthesis and antitumor activity of doxorubicin conjugated stearic acid-g-chitosan oligosaccharide polymeric micelles. *Biomaterials* **2009**, *30*, 6955–6963. [[CrossRef](#)] [[PubMed](#)]
50. Shen, W.C.; Ryser, H. Cis-aconityl spacer between daunomycin and macromolecular carriers: A model of ph-sensitive linkage releasing drug from a lysosomotropic conjugate. *Biochem. Biophys. Res. Commun.* **1981**, *102*, 1048–1054. [[CrossRef](#)]

51. Hong, S.; Leroueil, P.R.; Majoros, I.J.; Orr, B.G.; Baker, J.R., Jr.; Banaszak Holl, M.M. The binding avidity of a nanoparticle-based multivalent targeted drug delivery platform. *Chem. Biol.* **2007**, *14*, 107–115. [[CrossRef](#)] [[PubMed](#)]
52. Shi, X.; Lee, I.; Chen, X.; Shen, M.; Xiao, S.; Zhu, M.; Baker, J.R., Jr.; Wang, S.H. Influence of dendrimer surface charge on the bioactivity of 2-methoxyestradiol complexed with dendrimers. *Soft Matter* **2010**, *6*, 2539–2545. [[CrossRef](#)] [[PubMed](#)]



© 2018 by the authors. Licensee MDPI, Basel, Switzerland. This article is an open access article distributed under the terms and conditions of the Creative Commons Attribution (CC BY) license (<http://creativecommons.org/licenses/by/4.0/>).